Preparation and evaluation of spray dried rosuvastatin calcium-PVP microparticles for the improvement of serum lipid profile

Ramadan Al-Shdefat[a,**], Md Khalid Anwer[b,*], Mohamed H. Fayed[b], Badar B. Alsulays[b], Hesham M. Tawfeek[c], Rehab F. Abdel-Rahman[d], Gamal A. Soliman[e,f]

[a] Dept. of Pharmaceutical Sciences, Faculty of Pharmacy, Jadara University, Irbid, Jordan
[b] Dept. of Pharmaceutics, College of Pharmacy, Prince Sattam Bin Abdulaziz University, Al-Kharj, 11942, Saudi Arabia
[c] Department of Industrial Pharmacy, Faculty of Pharmacy, Assiut University, Assiut, Egypt
[d] Department of Pharmacology, National Research Centre, Giza, Egypt
[e] Department of Pharmacology, College of Veterinary Medicine, Cairo University, Giza, Egypt
[f] Department of Pharmacology, College of Pharmacy, Prince Sattam Bin Abdulaziz University, Al-Kharj, Saudi Arabia

ARTICLE INFO

ABSTRACT

The poor physicochemical properties of rosuvastatin calcium (ROS) remains a challenge for dosage form development. In the present study, we explore the development of spray dried ROS loaded PVP microparticles to improve the release of ROS as well as the anti-hyperlipidemic efficacy. The ROS loaded PVP microparticles (F1–F3) were developed by spray drying method with a range of particle size (1.26–1.67 μm), PDI (0.138-0.267), PDE (78 ± 3.2 to 89 ± 4.1%), PDL and (14.8 ± 1.2 to 39.4 ± 3.3%). The ROS loaded microparticles (F3) was optimized based on preliminary characterization and further evaluated for DSC, FTIR, SEM, in vitro release studies and anti-hyperlipidemic activity. Overall, It was proved that spray dried PVP microparticles was efficient carrier to deliver rosuvastatin with improved serum lipid profile of hyperlipidemic rats.

1. Introduction

Rosuvastatin calcium (ROS) belongs to a class of cholesterol-lowering drugs called HMG-CoA reductase inhibitors (statins). It reduces the production of cholesterol in the liver by inhibiting the activation of the HMG-CoA reductase enzyme that is responsible for cholesterol synthesis in the body [1,2]. ROS is used to lower LDL (low-density lipoprotein, bad cholesterol), raise HDL (high-density lipoprotein, good cholesterol), and lower triglycerides in the blood [3,4]. It is used along with a proper diet (low in fats and cholesterol) and exercise to slow the progress of cardiovascular disease and helps to prevent heart attacks and strokes. ROS belongs to the class II biopharmaceutical classification system (BCS) which is characterized by a poorly water soluble drug and the rate of its oral absorption is often limited by the dissolution rate in the gastrointestinal tract [5–7]. The absolute bioavailability of ROS is approximately 20% due to its extensive first pass metabolism and poor aqueous solubility [8–10].

Polyvinylpyrrolidone (PVP) is a synthetic, hygroscopic, amorphous water-soluble polymer composed of the monomer N-vinylpyrrolidone. It has been used successfully for decades in formulations development due to their ability to dissolve in both water and non-aqueous solvents. It is used as a binder in many pharmaceutical tablets and capsules, sugar and film coating, lubricant and film former in ophthalmic solutions, and as an adhesive for transdermal systems [11,12]. It is also used in many other applications with various roles as an adhesive, additive, and emulsifier. PVP is available in four viscosity grades, they are characterized by K-value (Fikentscher K value): K-15, K-30, K-60, K-90, with the average molecular weight being 10000, 40000,160000, and 360000, respectively. The molecular weight of polymers PVP are often reported in terms of the Fikentscher K-value that derived from a solution viscosity. Polyvinylpyrrolidone is a cross-linkable to a water insoluble drug either in the course of vinylpyrrolidone polymerization, by addition of an appropriate multifunctional comonomer or by post-reaction, typically through hydrogen abstraction chemistry [13,14]. Spray drying is the technique used for the conversion of liquids such as slurries, emulsion, and dispersion, into solid particles with preferred size, porosity, shape, density and distribution. The spray drying are used to control the size, shape, porosity and solubility enhancement of poorly soluble drugs [15].

The purpose of this study to prepare spray dried ROS loaded PVP

Table 1
Formulation of Rosuvastatine - Polyvinylpyrrolidone microparticles.

Formulations	Drug:PVP (w/w)	Chloroform:ethanol (v/v)	Percent yield
F1	1:1	30 : 10	50
F2	1:3	30 : 30	44
F3	1:5	30 : 50	71

microparticles that could have a potential to enhance the bioavail-ability. The developed microparticles may be suitable for the treatment of hyperlipidemic conditions.

2. Materials and methods

2.1. Materials

Rosuvastatin calcium (ROS), (98% purity) and Polyvinylpyrrolidone (PVP), (95%,purity) were obtained as a generous gift from a Jazeera Pharmaceutical Industries (JPI) Riyadh, Saudi Arabia. All chemicals and solvents used in this study were of analytical grade. Freshly prepared double distilled water was used throughout the work.

2.2. Preparation of ROS loaded PVP microparticles

A solution of ROS and PVP in a ratio of 1:1, 1:3 and 1:5 w/w were prepared by dissolving the required quantity of ROS in chloroform and PVP in ethanol. Table 1 represents the exact composition of each of the prepared formulae. The prepared two solutions were mixed and soni-cated in the ultrasonic bath for 5 min. The solution thus obtained was then spray dried (Büchi Mini Spray dryer B-290, Flawil, Switzerland) using the following optimized conditions - flow rate: 550 L/h, inlet temperature of 50 ± 3 °C, outlet temperature of 28 ± 2 °C, an aspirator rate of 100% and solution feed rate of 25% [16]. The spray dried microparticles were then weighed and the production yield of the microparticles was calculated using the following formula:

Percent yield = (the amount of microparticles obtained (g)/the theoretical amount (g) of non volatile material) x 100.

2.3. Measurement of mean particle size and polydispersity index (PDI)

The mean particle size and *PDI* were measured with the help of Microtrac particle size analyzer "Microtrac S3500 (Microtrac GmbH, Krefeld Germany)". Briefly, different microparticles (F1–F3) were dispersed in distilled water and sonicated for 15 min. The mean particle size and *PDI* for each formulae were measured [17].

2.4. Determination of percent drug entrapment (PDE) and percent drug loading (PDL)

The PDE and PDL of spray dried ROS-AVP microparticles (F1–F3) were measured directly by dissolving 100 mg of each microparticles in ethanol:water (50:50 v/v), and sonicated for 10 min. The content of drug was analyzed by UV spectroscopy at 243 nm after suitable dilution [18].

The amount of percent drug loading was calculated using following equation.

PDE = W – w / W *100

"Where W = theoretical amount of ROS; w = observed amount of ROS"

PDL = ROS present in microparticle / total weight of microparticles

2.5. Differential scanning calorimetry (DSC)

DSC thermal behavior of the optimized micropaticles samples (F3) were analyzed using a "Shimadzu DSC-60 (Shimadzu Corporation, Tokyo, Japan)". The samples were weighed accurately (5 mg) and put in a sealed aluminum crucibles. An empty aluminum crucibles/pan sealed was used as a reference. The samples were analyzed at a scanning rate of 10 °C min^{-1} from the temperature 25 to 250 °C in inert nitrogen environment (flow 15 mL min^{-1}).

2.6. Fourier transform infrared spectroscopy (FTIR)

The FTIR spectra of ROS calcium and microparticles (F3) were recorded on "ALPHA FT-IR Spectrometer, OPTIK, USA" using the potassium bromide pellet technique. The samples were mixed with potassium bromide (1:100) in a small clean glass mortar, then compressed to a transparent pellet by applying suitable pressure. Baseline was corrected by using blank potassium bromide pellet and the samples spectral scanning were done against a blank KBr pellet background at a wave number in the range of 4000–400 cm^{-1}.

2.7. Scanning electron microscopy (SEM)

The morphology of the pure ROS and ROS-PVP microparticle (F3) were observed using "SEM Microscope (Zeiss EVO LS10, Cambridge, UK)". The suspended sample was vortexed for 1 min and one drop of the suspension was spread on a slide and dried. Sample was mounted on stubs using adhesive carbon tape and coated under vacuum with gold in a sputter coater unit from "Quorum Technologies Ltd. (East Sussex, UK)" in an argon atmosphere. The sample was then scanned and photomicrographed.

2.8. In vitro release study

Drug release studies of prepared microparticles were performed using USP-2 dissolution apparatus. Briefly, ROS pure drug and spray dried ROS-PVP (1:1, 1:3 and 1:5, w/w) microparticles were dispersed in 900 mL media containing phosphate buffer (pH-6.8), and paddle was set at speed of 50 rpm, and temperature at 37 ± 2 °C. Five milliliter of each sample were withdrawn at specified time interval (0.5, 1, 2, 3, 6 & 9 h), and same dissolution media was compensated to keep the dissolution medium constant. The collected sample was analyzed for the drug content by UV spectroscopy at 243 nm [18].

2.9. Release kinetics of ROS from optimized microparticles

The obtained release data were evaluated by fitting in various kinetic models "(zero order, First order, Higuchi, Hixon-Crowell, Krosmeyer-Peppas)" to know the release pattern [19,20]. These models are expressed with following Equations.

Zero Order

$$Q_t = Q_0 + K_0 t \tag{1}$$

First Order

$$Log\ C = Log\ C_0 - K_1 t\ /\ 2.303 \tag{2}$$

Higuchi

$$Q_t = K.t^{0.5} \tag{3}$$

Hixon-Crowell

$$(W_0^{1/3} - W_t^{1/3}) = k_h.t \tag{4}$$

Krosemeyer-Peppas

$$Q_t\ /\ Q_\infty = k_p t^n \tag{5}$$

The symbols, Q_0, Q_t and Q_∞ are the amounts of ROS released initially, at time t and at infinite, respectively. However, C_0, C are the concentration of ROS in micropaticles initially and at time t respectively. The symbole W_0, and W_t are the amounts of ROS in microparticles initially and time t, respectively. The symbols k_0, k_1, k, k_h and k_p are the rate constants for zero order, first order, Higuchi, Hixon-Crowell and Krosemeyer-Peppas models, respectively. The symbole n represents the diffusion coefficient, a useful parameters of drug release mechanism.

2.10. Animal study

2.10.1. Animals

Twenty four male Wistar rats, at 5-weeks-old were obtained from the Animal House Colony at the National Research Centre (NRC), Egypt. The animals were housed in polypropylene cages under controlled ambient temperature of $25 \pm 2\,°C$ with $60 \pm 5\%$ relative humidity and a 12 h light/dark cycle. They had free access to food and water as well. The experimental procedures were complied with the National Institutes of Health Guide for the Care and were performed according to the protocol approved by the Institutional Medical Research Ethics Committee at the National Research Centre (approval number: MREC-18-188).

2.10.2. Experimental protocol

In vivo studies were performed on four groups of animals; each group was consisted of six rats. The total duration of the experiment was kept ten weeks for both experimental and control groups. At the end of the sixth week, hyperlipidemia was developed and the treatment begun for 4 weeks (Table 2). Rosuvastatin (ROS) was given to rats orally in a dose of 3 mg/kg, while ROS-PVP (F3) microparticles was given in a dose of 18 mg/kg, taking in consideration that 6 g of the F3 microparticles containing 1 g of ROS.

A normal control group (NC, n = 6) was given free access to water and standard chow diet (Al-Marwa for Animals Feed Manufacturing, Egypt) containing 19.80% protein, 39.25% carbohydrate, 4.41% fat, 13.25% fiber. In order to study the effects of ROS and F3 microparticles on high fat diet (HFD) condition, a group of rats (n = 18) received water and a HFD containing 15.30 g protein, 43.34 g carbohydrate, 11.86 g fat, 10.20 g fiber per 100 g chow.

The HFD was formulated by mixing the supplemented ingredients with a previously triturated standard chow. The dietary ingredients were homogenized in 60 °C warm distilled water and the homogenate was used to prepare the pellets. Therefore, both control and experimental diet were given fresh each day as dry pellets, and there was no spillage. The HFD was obtained by mixing 848 mL soy oil, 1310 g sucrose, 123 g cholesterol and 12 g cholic acid to 1000 g of the standard chow [21].

After 6 weeks of the experimental period, the HFD group was randomly divided into three subgroups (n = 6/group): (HC) group remained receiving HFD and water, (ROS) group given HFD and ROS at 3 mg/kg and (ROS-PVP) group given HFD and F3 microparticles at 18 mg/kg.

Table 2
Animal groups and respective treatments.

	Groups	Diet (0–6 week)	Treatment (7–10 week)
1	Normal control group (NC)	NCD	NCD
2	Hyperlipidemic control group (HC)	HFD	HFD
3	Rosuvastatin group (ROS)	HFD	(HFD) + (ROS)
4	ROS-PVP (F3)	HFD	(HFD) + (F3)

NCD: normal chow diet, HFD: high fat diet, ROS: treatment with rosuvastatin, F3: treatment with Rosuvastatin-Polyvinylpyrrolidone microparticles.

ROS and F3 microparticles were gavaged (orally intubated) after suspending in0.5 mL of distilled water. Treatments were administered once a day for four weeks. The body weights were determined at the beginning of the experiment (0-time) and at the ends of the 6th and 10th weeks.

2.10.3. Sample collection

At the end of the experimental period, rats were fasted for 10–12 h, with free access to water, and then were anesthetized through intraperitoneal injection of sodium pentobarbital. Blood samples (2 mL) were collected from inferior vena cava and centrifuged at 3000 rpm (1008 rcf) for 15 min to separate serum. The livers were removed immediately by dissection, washed in ice-cold saline and blotted between two filter papers to eliminate the surface water.

2.10.4. Serum biochemical analysis

Fasting blood samples were taken for measurement of the serum concentrations of glucose, triglycerides (TG), total cholesterol (TC) and high density lipoprotein cholesterol (HDL-C). Measurements were carried out using enzymatic colorimetric methods by commercially available kits (Quimica Clinica, Spain). The low-density lipoprotein cholesterol (LDL-C) and very low-density lipoprotein cholesterol (VLDL-C) were calculated according to the method of Friedewald et al. (1972) [22]: LDL-C = TC − (HDL-C + TG/5) and VLDL-C = TG/5. Atherogenic index (AI) was calculated using the formula of Kayamori and Igarashi (1994) [19]: AI = (TC-HDL-C)/HDL-C.

The levels of alanine transaminase (ALT), aspartate aminotransferase (AST), alkaline phosphatase (ALP) and gamma glutamyl transferase (γ-GT) in the sera were determined using commercial diagnostic kits (Chema Diagnostica, Italy).

2.10.5. Liver index and liver histological examination

Liver index was calculated from the ratio of liver weight to body weight [23]. Liver index = (Liver weight/Body weight) × 100. The removed livers were fixed in 10% neutral-buffered formaldehyde for further histological study. The tissues were embedded in paraffin and cut into 5 μm thick sections and subsequently stained by hematoxylin and eosin (H&E) for histological examination (n = 3).

2.11. Statistical analysis

Statistical evaluations were determined using one way ANOVA followed by LSD post hoc test using SPSS 16 software. Any differences between the groups were considered significant at $p \leq 0.05$ level. All data were displayed as the mean ± SEM of values obtained from six rats.

3. Results and discussion

3.1. Measurement of mean particle size and PDI

The mean particle size and PDI of all developed microparticles (F1–F3) are tabulated in Table 3. The amount of PVP polymer directly influence on the size of microparticles. The highest mean particle of F3 (1.67 μm) was measured among all formulae, It could be due to large

Table 3
Evaluation of the particle size, PDI and PDL of microparticles.

Formulae	Particle size (μm)	PDI	PDE	PDL
F1	1.26 ± 0.24	0.237	78 ± 3.2	39.4 ± 3.3
F2	1.42 ± 0.34	0.138	82 ± 5.4	20.5 ± 1.5
F3	1.67 ± 0.48	0.267	89 ± 4.1	14.8 ± 1.2

PDI – Polydispersity Index; PDE – Percent drug entrapment; PDL – Percent drug loading.

content of PVP present in F3 formulae. The *PDI* is a measure of width of dispersion of particles, the values less than 0.3 is considered as monodisperse and homogenous particles [24]. The PDI of all the microparticles (F1–F3) showed a narrow dispersion (*PDI*, 0.138–0.267), thus it can be considered as monodisperse [25].

3.2. Determination of percent drug entrapment (PDE) and percent drug loading (PDL)

The amount of ROS incorporated inside the PVP polymer was evaluated as the percent drug entrapment and percent drug loading as tabulated in Table 3. The PDE and PDL of ROS in the PVP microparticles (F1–F3) were measured in the range of 78–89% and 14.8–39.4%, respectively. It is evident from the result that an increase in PVP polymer content in F3 leads to an increase in percent drug entrapment, this is probably due to higher viscosity of polymer that resistance in diffusion of drug from PVP polymer [26,27]. Based on particle size (1.67 μm), *PDI* (0.267), PDE (89%) and PDL (14.8%), F3 formulae was found optimum and further evaluated.

3.3. DSC studies

Thermal behavior of the pure ROS compared with the thermograms of optimized microparticles (F3) in the temperature range of 25–250 °C is shown in Fig. 1. The thermogram of the pure ROS showed a sharp endothermic peaks corresponding to 144.18 °C, which was in agreement with those reported in literature [28]. As we can see the DSC thermogram of ROS-PVP microparticles (F3), the peak of ROS was completely disappeared. It may be due to presence of PVP polymer in the formulation. This clearly revealed that the ROS was completely entrapped and protected inside the PVP polymeric matrix.

3.4. FTIR studies

FTIR spectra of pure ROS and optimized microparticles (F3) were recorded to confirm the entrapment of drug within the PVP polymer. The characteristic FT-IR peaks of ROS calcium were observed in the region of 3269.72, 3046.01, and 1406.82 cm^{-1} due to cyclic amine, C–H stretching, C=O stretching and O–H bending (Fig. 2) [29]. Significant changes could be seen in the spectra of ROS loaded PVP microparticles, all the characteristic peaks of ROS were reduced in intensity significantly in the finger print region of ROS, which indicated

complete entrapment of ROS inside the PVP polymer.

3.5. SEM images

The SEM image of the pure ROS calcium and optimized ROS loaded PVP microparticles (F3) is shown in Fig. 3. It could be seen from the image that the prepared microparticles are irregular in shape with smooth surface. From the image, it is clearly obvious that the microparticles were agglomerated. The result obtained through SEM showed an average particle size approximate to 1.67 μm, in close approximation with that obtained by dynamic light scattering technique (DLS).

3.6. In vitro release studies

The drug release profile of pure ROS and optimized spray dried microparticles (F3) are shown in Fig. 4. It was reported that solubility of ROS is maximum at higher pH [29], so, release studies of the micropaticles has been performed in phosphate buffer (pH 6.8). A significant increased in release of microparticles could be seen in comparison with pure ROS. A rapid release of ROS (88.8%) was observed in first 3 h of the study probably due to the surface adsorbed drug on microparticles. The remaining amount of drug from the microparticles was released slowly in next 6 h. Spray drying micronized particles easily diffuses to the media due to larger surface area. The enhanced release of ROS may be helpful in reducing the frequency of oral administration of drug. The release data were fitted to different kinetic models to know the release mechanism of drug from microparticles. The data was consistently fitted to Krosemeyer-Peppas model with value of R^2 ≥ 0.9963.

3.7. Effects on body weight gain and relative liver weight

High fat diet is one of most commonly used environmental factors associated with the induction of obesity in rats. As shown in Table 4, consumption of HFD for six weeks led to significant increase in body weight gain of rats compared to NC animals. This effect could be attributed to an imbalance of carbohydrate, protein, and fat metabolism [30].

After another 4 weeks, a more apparent difference in body weight gain between the HC group (113.8 ± 5.57 g) and the NC group (63.5 ± 2.58 g; $p ≤ 0.05$) was observed. Treatment of rats with ROS or F3 microparticles significantly reduced their body weight gain compared to HC group. Importantly, the hyperlipidemic rats treated with
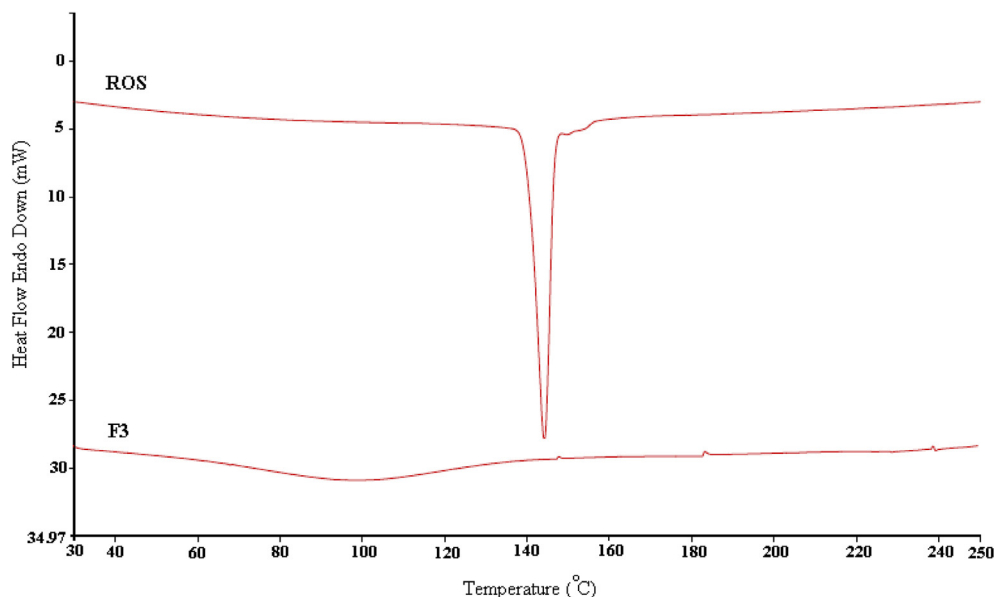
Fig. 1. DSC spectra of the pure ROS compared with the thermograms of microparticles (F3).
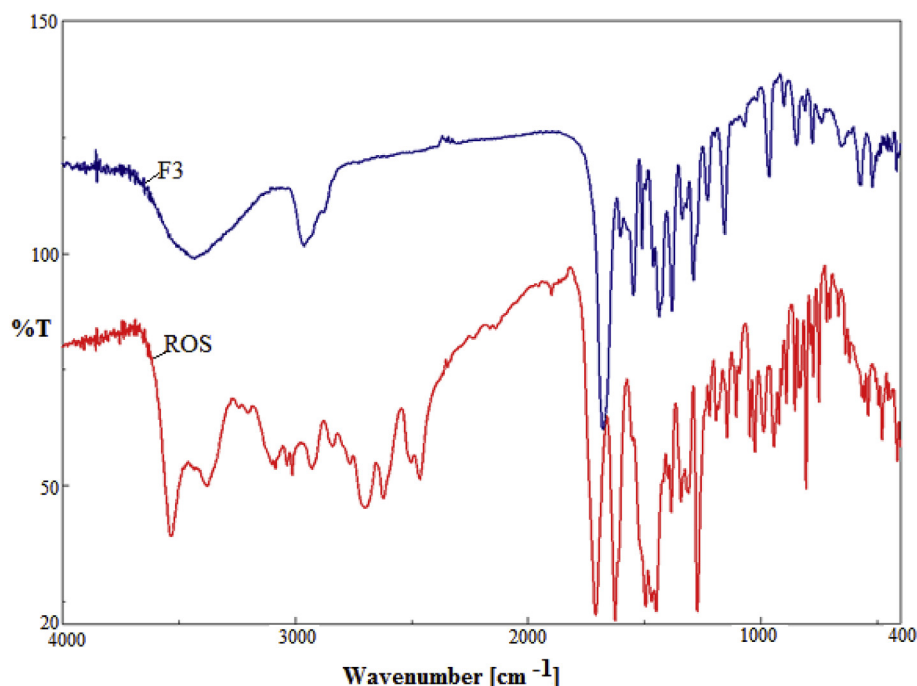
Fig. 2. FTIR spectra of the pure ROS compared with the microparticles (F3).
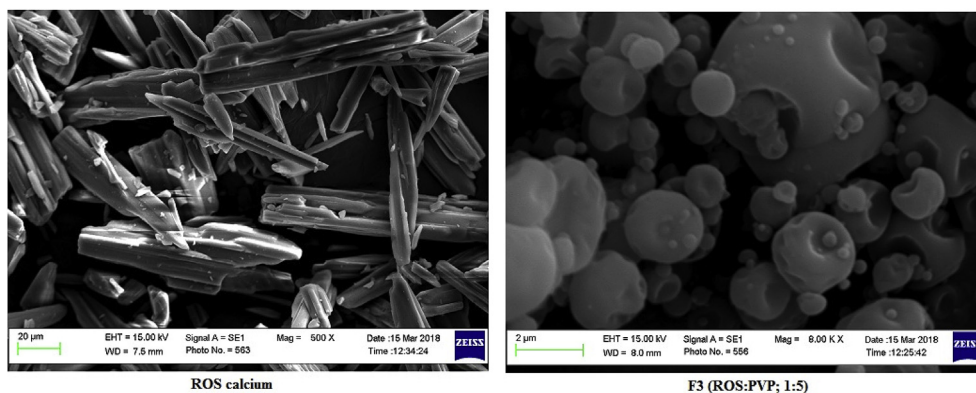
Fig. 3. SEM images of the pure ROS compared with the microparticles (F3).

the F3 microparticles achieved a more significant reduction in their body weight gain compared with those received ROS monotherapy. The F3 microparticles brought back the body weight gain (71.2 ± 3.60 g) towards normal value (63.5 ± 2.58 g).

Likewise, liver weight was significantly increased in HC rats and in groups treated with ROS or F3 microparticles compared to NC animals (Table 5). The rats treated with ROS and F3 microparticles showed a significant decrease ($p \leq 0.001$) in liver weight than the HC rats. Furthermore, liver index was significantly increased in HC group (4.38 ± 0.32) compared to NC (2.51 ± 0.11). However, ROS and F3 microparticles decreased the liver index in hyperlipidemic rats by 13.9% and 30.4%, respectively compared with HC. F3 microparticles was more effective than ROS mono therapy in controlling liver weight and liver index in hyperlipidemic rats. The effectiveness of the microparticles was confirmed as it was successfully reversed the increased liver index of hyperlipidemic rats toward their normal values.

3.8. Effects on blood glucose and serum lipid profile

Around 70% of patients with nonalcoholic steatohepatitis have concurrent dyslipidemia, making treatment with lipid-lowering agents appear to be a targeted approach [30]. Statins are the current treatment

of choice to avoid vascular complications in diabetics with hypercholesterolemia [31].

A high cholesterol and LDL levels, along with decreased HDL level is a key role in atherosclerosis progression, whereas lipid-lowering compounds reduce the risk of atherosclerosis and coronary heart disease development [32].

In our study, marked improvements in blood glucose level and lipid profile were observed in hyperlipidemic rats medicated with ROS and F3 microparticles at the end of the experimental period compared to HC rats. Supporting our findings, reduction in the level of TG, TC and LDL of rats treated with ROS has been reported by other researchers [33,34].

On intergroup comparison, F3 microparticles showed a better improvement in blood glucose level and lipid profile than ROS monotherapy. Administering this F3 microparticles to hyperlipidemic rats tends to bring their serum lipid profile to normal values. This result revealed the beneficial effect of the microparticles against hyperlipidemia. Atherogenic index was significantly reduced in hyperlipidemic rats administered ROS (2.71 ± 0.18) and ROS-PVP (1.48 ± 0.11) when compared to HC group (4.84 ± 0.25) (Table 6).
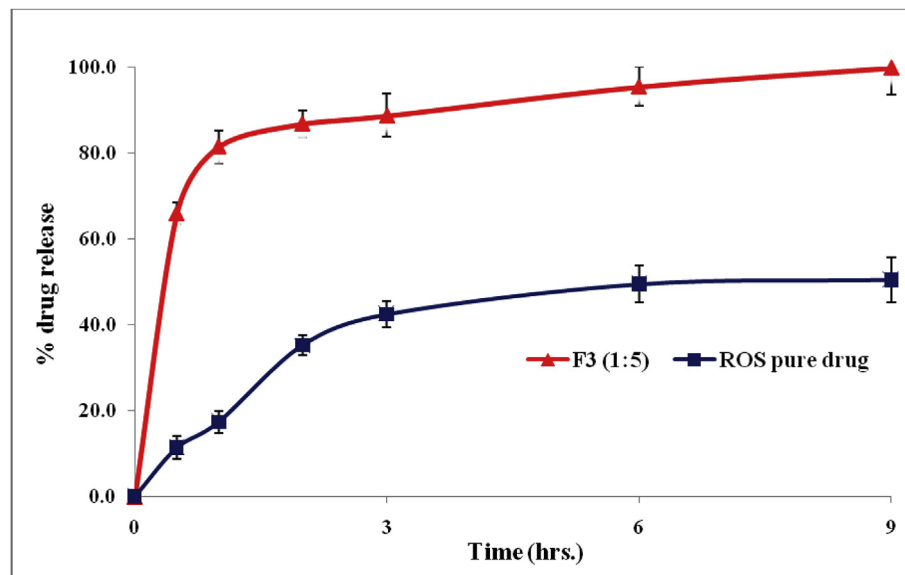
Fig. 4. In vitro drug release of the pure ROS compared with the microparticles (F3).

Table 4
Effect of ROS and F3 microparticles on body weight gain of rats fed a high-fat diet (HFD).

Treatment Groups	Body weight (g)				
	0-time	6-weeks	Body weight gain(g)	10-weeks	Body weight gain (g)
NC	150.2 ± 5.83	264.8 ± 5.48[b]	114.6 ± 5.18[b]	328.3 ± 6.94[bc]	63.5 ± 2.58[bc]
HC	151.3 ± 6.15	345.8 ± 6.15[a]	194.5 ± 7.25[a]	459.6 ± 7.73[a]	113.8 ± 5.57[a]
ROS	153.8 ± 6.22	340.2 ± 6.24[a]	186.4 ± 6.41[a]	434.8 ± 5.85[ab]	94.6 ± 4.22[ab]
F3	149.7 ± 5.59	343.5 ± 5.37[a]	193.8 ± 7.73[a]	414.7 ± 6.39[abc]	71.2 ± 3.60[bc]

[a]$P \leq 0.05$, statistically significant in comparison with the normal control (NC) group.
[b]$P \leq 0.05$, statistically significant in comparison withthe hyperlipidemic control (HC) group.
[c]$P \leq 0.05$, statistically significant in comparison with rosuvastatin(ROS) group.

Table 5
Effect of ROS and F3 microparticles on the relative liver weight of rats fed a high-fat diet (HFD).

Treatment Groups	Liver weight (g)	Liver index
NC	7.2 ± 0.47[bc]	2.51 ± 0.11[bc]
HC	12.5 ± 0.85[ac]	4.38 ± 0.32[ac]
ROS	10.6 ± 0.62[ab]	3.77 ± 0.21[ab]
F3	8.4 ± 0.69[abc]	3.05 ± 0.29[bc]

[a]$P \leq 0.05$, statistically significant in comparison with the normal control (NC) group.
[b]$P \leq 0.05$, statistically significant in comparison withthe hyperlipidemic control (HC) group.
[c]$P \leq 0.05$, statistically significant in comparison with rosuvastatin(ROS) group.

3.9. Effects on liver function

The liver is the central organ for lipid metabolism. Estimation of serum ALT andAST is a reflection of damage to the structural integrity ofthe liver [35]. In the present study, the increased activity of ALT, AST, ALPand γ-GTenzymes in serum of HC rats reflects their liver injury. Treatment with ROS and F3 microparticles significantly decreased the elevated liver markers enzymes compared to HC group. These findings are in accordance with those obtained by Antonopoulos et al. (2006) and Seif el-Din et al. (2015) [30,36], where ROS treatment in hyperlipidemic patients and rat model, respectively resulted in normalization of γ-GTwith significant decrease in ALT, AST and ALP levels (Table 7).

3.10. Macroscopic and microscopic examinations of liver

The visual appearance of healthy livers of the NC group revealed normal redness (Fig. 5A). Consumption of HFD for six weeks led to

Table 6
Effect of ROS and F3 microparticles on the lipid profile of rats fed a high-fat diet (HFD).

Treatment Groups	Glucose (mg/dL)	TG (mg/dL)	TC (mg/dL)	HDL (mg/dL)	LDL (mg/dL)	VLDL (mg/dL)	AI
NC	78.1 ± 3.25[bc]	51.6 ± 3.46[bc]	70.9 ± 3.76[bc]	33.6 ± 1.88[bc]	26.9 ± 1.12[bc]	10.32 ± 0.52[bc]	1.11 ± 0.1[bc]
HC	161.3 ± 5.84[ac]	94.7 ± 4.28[ac]	101.0 ± 4.84[ac]	17.3 ± 0.52[ac]	64.7 ± 3.25[ac]	18.94 ± 0.86[a]	4.84 ± 0.25[a]
ROS	104.9 ± 4.71[ab]	81.4 ± 3.55[ab]	82.0 ± 3.32[ab]	22.1 ± 0.75[ab]	43.6 ± 1.74[ab]	16.28 ± 0.73[ab]	2.71 ± 0.18[ab]
F3	82.1 ± 3.76[bc]	61.7 ± 3.2[bc]	71.4 ± 3.15[bc]	28.8 ± 1.16[bc]	30.2 ± 1.27[bc]	12.34 ± 0.77[bc]	1.48 ± 0.11[abc]

[a]$P \leq 0.05$, statistically significant in comparison with the normal control (NC) group.
[b]$P \leq 0.05$, statistically significant in comparison withthe hyperlipidemic control (HC) group.
[c]$P \leq 0.05$, statistically significant in comparison with rosuvastatin(ROS) group.

Table 7

Effect of ROS and F3 microparticles the liver function of rats fed a high-fat diet (HFD).

Treatment Groups	ALT (U/L)	AST (U/L)	ALP (U/L)	γ-GT (U/L)
NC	54.8 ± 2.23[bc]	117.3 ± 4.18[bc]	183.3 ± 6.95[bc]	15.5 ± 0.84[bc]
HC	127.5 ± 4.94[a]	225.2 ± 8.46[a]	315.2 ± 9.77[a]	37.1 ± 1.40[a]
ROS	79.6 ± 3.75[ab]	156.3 ± 5.50[ab]	243.1 ± 8.65[ab]	26.5 ± 0.88[ab]
F3	62.8 ± 2.88[bc]	130.2 ± 4.72[bc]	205.4 ± 8.20[bc]	18.2 ± 0.92[bc]

[a] $P \leq 0.05$, statistically significant in comparison with the normal control (NC) group.

[b] $P \leq 0.05$, statistically significant in comparison withthe hyperlipidemic control(HC) group.

[c] $P \leq 0.05$, statistically significant in comparison with rosuvastatin(ROS) group.
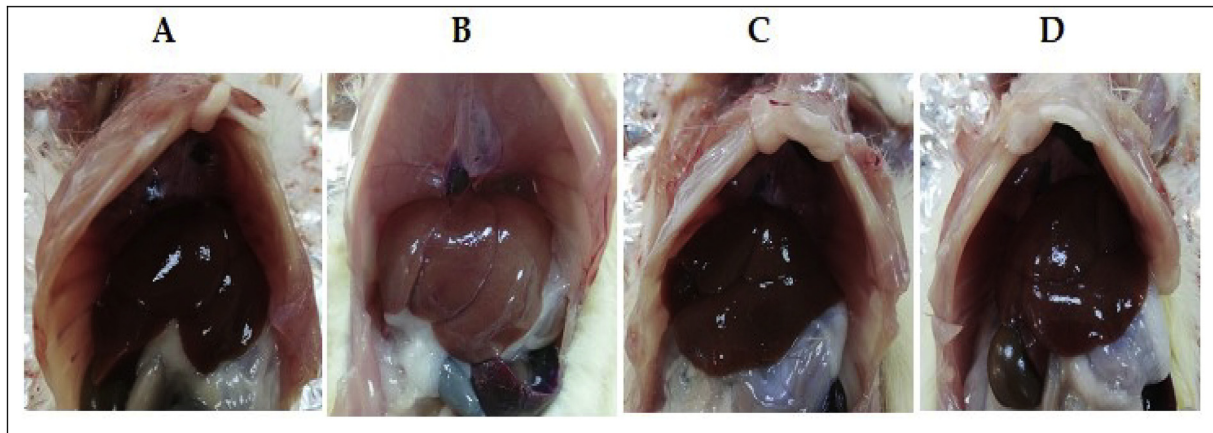
Fig. 5. Liver gross appearance, A: normal control, B: hyperlipidemic control, C: ROS treated, D: F3 microparticles treated.
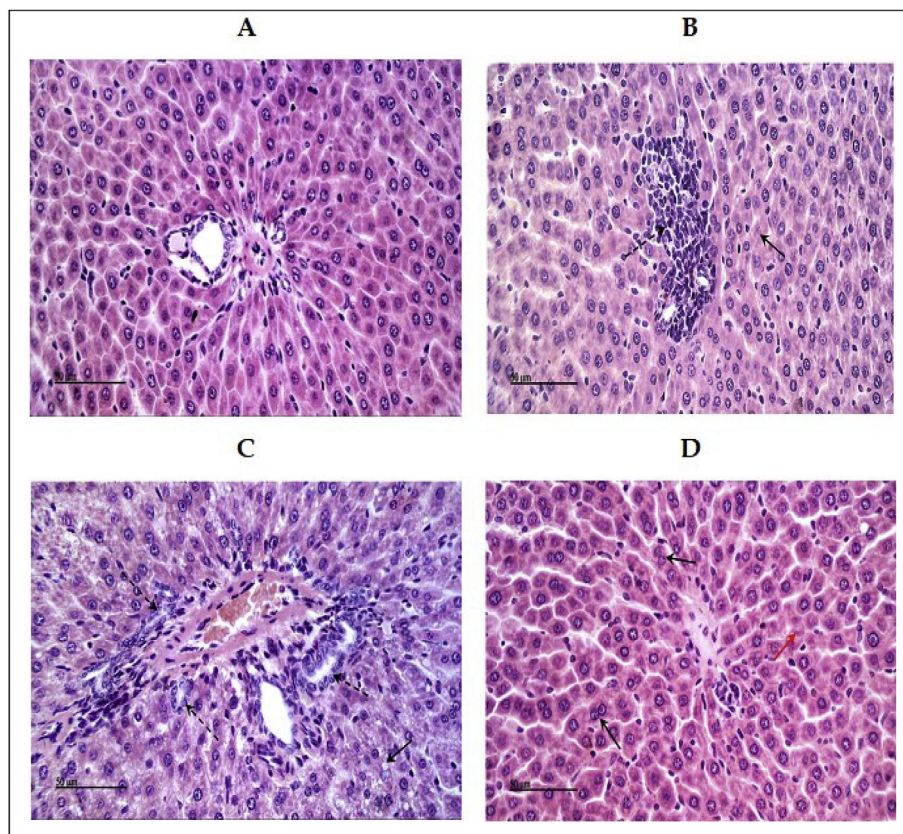
Fig. 6. Liver histological staining using H&E (magnification 20×), A: normal control, B: hyperlipidemic control, C: ROS treated, D: F3 microparticles treated.

enlarged and pale appearance of liver (Fig. 5B–D). Treatment of rats with ROS and F3 microparticles improved the gross appearance of liver tissue from pale red to a more reddish color (Fig. 5C and D).

As depicted in Fig. 6, the microscopic examination of liver tissue samples of NC rats revealed normal morphological appearance of hepatic parenchyma with almost apparent intact hepatocytes as well as intact hepatic blood vessels (Fig. 5A). HC rats showed pericentral microvesicular steatosis with scattered multiple foci of necrotic tissue replaced with inflammatory cells, moderate degenerative changes of some hepatocytes (arrow), marked activation of kupffer cells as well as periportal inflammatory cells infiltrates (dashed arrow) (Fig. 6B). Liver samples of ROS group showed diffuse moderate vacuolar degeneration of hepatocytes with minimal fatty changes (arrow), mild periportal inflammatory cells infiltration with proliferation of bile ducts (dashed arrow) (Fig. 6C). F3 microparticles group showed the most protected samples with many apparent intact hepatocytes with occasional binucleated cells (arrow) and fewer degenerated cells, sporadic mild focal perivascular aggregation of inflammatory cells (dashed arrow), many activated kupffer cells. Sporadic dilatation of hepatic sinusoids was also recorded (Fig. 6D).

The obtained data showed that feeding rats with HFD resulted in the progression of hepatic steatosis and increased liver index. However treating rats with ROS or F3 microparticles inhibited the progression of hepatic steatosis in rats. Histological findings together with the other findings in our study confirmed the greater effect of F3 microparticles than ROS alone. These outcomes suggest that an improvement in physicochemical characteristics of ROS could enhance its therapeutic efficiency.

4. Conclusion

In this study, spray dried ROS loaded PVP microparticles (F1–F3) were prepared by differing PVP concentrations (ROS:PVP; 1:1, 1:3 & 1:5). The optimized microparticles (F3) had a suitable size and entrapment efficiency to enhance the efficacy of drug, which was confirmed by *in vitro* release and anti-hyperlipidemic studiers. Hence, it is concluded that the developed micropaticles benefits from its micro size and promise a better therapeutic efficacy. Our findings offer a vision into the greater performance of F3 microparticles compared to the pure drug, in preventing/reducing the deleterious effects of HFD on liver tissue and in improving the serum lipid profile of hyperlipidemic rats.

Declaration of competing interest

The authors report no conflict of interest associated with the article.

Acknowledgement

References

[1] Drugbank of Rosuvastatin Calcium, DB01098. Citation date 1/1/2017.

[2] D.H. Alshora, M.A. Ibrahim, E. Elzayat, O.T. Almenazel, F. Alanazi, Rosuvastatin calcium nanoparticles: improving bioavailability by formulation and stabilization codesign, PLoS One 13 (2018) e0200218.

[3] N. Dudhipala, K. Veerabrahma, Improved anti-hyperlipidemic activity of Rosuvastatin Calcium via lipid nanoparticles: pharmacokinetic and pharmacodynamic evaluation, Eur. J. Pharm. Biopharm. 110 (2017) 47–57.

[4] M.R. Hirpara, J. Manikkath, K. Sivakumar, R.S. Managuli, K. Gourishetti, N. Krishnadas, R.R. Shenoy, B. Jayaprakash, C.M. Rao, S. Mutalik, Long circulating PEGylated-chitosan nanoparticles of rosuvastatin calcium: development and in vitro and in vivo evaluations, Int. J. Biol. Macromol. 107 (2018) 2190–2200.

[5] R.M. Sarfraz, M. Ahmad, A. Mahmood, M.R. Akram, A. Abrar, Development of β-cyclodextrin-based hydrogel microparticles for solubility enhancement of rosuvastatin: an in vitro and in vivo evaluation, Drug Des. Dev. Ther. 11 (2017) 3083–3096.

[6] C.K. Thakur, N. Thotakura, R. Kumar, P. Kumar, B. Singh, D. Chitkara, K. Raza, Chitosan modified PLGA polymeric nanocarriers with better delivery potential for tamoxifen, Int. J. Biol. Macromol. 93 (Pt A) (2016) 381–389.

[7] C. Misra, N. Thotakura, R. Kumar, B. Singh, G. Sharma, O.P. Katare, K. Raza, Improved cellular uptake, enhanced efficacy and promising pharmacokinetic profile of docetaxel employing glycine-tethered C60-fullerenes, Mater. Sci. Eng. C Mater. Biol. Appl. 76 (2017) 501–508.

[8] P.D. Martin, P.D. Mitchell, D.W. Schneck, Pharmacodynamic effects and pharmacokinetics of a new HMG-CoA reductase inhibitor, rosuvastatin, after morning or evening administration in healthy volunteers, Br. J. Clin. Pharmacol. 54 (2002) 472–477.

[9] K. Balakumar, C.V. Raghavan, S. Abdu, Self-nanoemulsifying drug delivery system (SNEDDS) of rosuvastatin calcium: design, formulation, bioavailability and pharmacokinetic evaluation, Colloids Surf., B 112 (2013) 337–343.

[10] A. Mahmood, M. Ahmad, R.M. Sarfraz, M.U. Usman, β-CD based hydrogel microparticulate system to improve the solubility of acyclovir: optimization through in-vitro, in-vivo and toxicological evaluation, J. Drug Deliv. Sci. Technol. 36 (2016) 75–88.

[11] M. Teodorescu, M. Bercea, S. Morariu, Biomaterials of PVA and PVP in medical and pharmaceutical applications: perspectives and challenges, Biotechnol. Adv. 37 (2019) 109–131.

[12] X. Zhi, H. Fang, C. Bao, G. Shen, J. Zhang, K. Wang, S. Guo, T. Wan, D. Cui, The immunotoxicity of graphene oxides and the effect of PVP-coating, Biomaterials 34 (2013) 5254–5261.

[13] M. Teodorescu, M. Bercea, Poly(vinylpyrrolidone) – a versatile polymer for biomedical and beyond medical applications, Polym. Plast. Technol. Eng. 54 (2015) 923–943.

[14] K. Raza, Nanotechnology-based drug delivery products: need, design, pharmacokinetics and regulations, Curr. Pharmaceut. Des. 24 (2018) 5058.

[15] S. Ghanbarzadeh, H. Valizadeh, S. Yaqoubi, A. Asdagh, H. Hamishehkar, Application of spray drying technique for flowability enhancement of divalproex sodium, Drug Res. (Stuttg) 68 (2018) 168–173.

[16] R. Al-Shdefat, B.E. Ali, M.K. Anwer, M.H. Fayed, A. Alalaiwe, G.A. Soliman, Sildenafil citrate-Glycyrrhizin/Eudragit binary spray dried microparticles: a sexual behavior studies on male rats, J. Drug Deliv. Sci. Technol. 36 (2016) 141–149.

[17] F.I. Al-Saikhan, M.A. Abd-Elaziz, R. Al-Shdefat, M.K. Anwer, M.S. Iqbal, Preparation and evaluation of aviptadil acetate loaded Plga microparticles: a preliminary study to treat pulmonary hypertension, Lat. Am. J. Pharm. 38 (2019) 545–552.

[18] S. Naveed, F. Qamar, Simple UV spectrophotometric assay of rosuvastatin formulations, Global J. Pharm.Res. 3 (2014) 1985–1990.

[19] S.M. Alshahrani, A.S. Alshetaili, A. Alalaiwe, B.B. Alsulays, M.K. Anwer, R. Al-Shdefat, F. Imam, F. Shakeel, Anticancer efficacy of self-nanoemulsifying drug delivery system of sunitinib malate, AAPS PharmSciTech 19 (2018) 123–133.

[20] M.K. Anwer, M. Mohammad, E. Ezzeldin, F. Fatima, A. Alalaiwe, M. Iqbal, Preparation of sustained release apremilast-loaded PLGA nanoparticles: in vitro characterization and in vivo pharmacokinetic study in rats, Int. J. Nanomed. 14 (2019) 1587–1595.

[21] Y.S. Diniz, A.C. Cicogna, C.R. Padovani, L.S. Santana, L.A. Faine, E.L.B. Novelli, Diets rich in saturated and polyunsaturated fatty acids: metabolic shifting and cardiac health, Nutrition 20 (2004) 230–234.

[22] W.T. Friedewald, R.I. Levy, D.S. Fredrickson, Estimation of the concentration of low-density lipoprotein cholesterol in plasma, without use of the preparative ultracentrifuge, Clin. Chem. 18 (1972) 499–502.

[23] F. Kayamori, K. Igarashi, Effects of dietary nasunin on the serum cholesterol level in rats, Biosci. Biotechnol. Biochem. 58 (1994) 570–571.

[24] M. Danaei, M. Dehghankhold, S. Ataei, F. Hasanzadeh Davarani, R. Javanmard, A. Dokhani, S. Khorasani, M.R. Mozafari, Impact of particle size and polydispersity index on the clinical applications of lipidic nanocarrier systems, Pharmaceutics 10 (2018) E57.

[25] T.S. El-Alfy, M.H. Hetta, N.Z. Yassin, R.F. Abdel Rahman, E.M. Kadry, Estrogenic activity of Citrus medica L. leaves growing in Egypt, J. Appl. Pharm. Sci. 2 (2012) 180–185.

[26] W. Huang, C.P. Tsui, C.Y. Tang, L. Gu, Effects of compositional tailoring on drug delivery behaviours of silica xerogel/polymer core-shell composite nanoparticles, Sci. Rep. 8 (2018) 13002.

[27] A.S. Alshetaili, M.K. Anwer, S.M. Alshahrani, A. Alalaiwe, B.B. Alsulays, M.J. Ansari, F. Imam, S. Alsheri, Characteristics and anticancer properties of Sunitinib malate-loaded poly-lactic-co-glycolic acid nanoparticles against human colon cancer HT-29 cells lines, Trop. J. Pharm. Res. 17 (2018) 1263–1269.

[28] K.A. Dhoranwala, P. Shah, S. Shah, Formulation optimization of rosuvastatin Calcium Loaded solid lipid nanoparticles by 32 full-factorial design, Nano World J. 4 (2015) 112–121.

[29] R.M. Sarfraz, M. Ahmad, A. Mahmood, M.U. Minhas, A. Yaqoob, Development and evaluation of rosuvastatin calcium based microparticles for solubility enhancement: an InVitro study, Adv. Polym. Technol. 36 (2017) 433–441.

[30] S.H.S. Seif El-Din, N.M. El-Lakkany, A.A. El-Naggar, O.A. Hammam, H.A.A. El-Latif, A.A. Ain-Shoka, F.A. Ebeid, Effects of rosuvastatin and/or β-carotene on non-alcoholic fatty liver in rats, Res. Pharm. Sci. 10 (2015) 275.

[31] S. Ludwig, G.X. Shen, Statins for diabetic cardiovascular complications, Curr. Vasc. Pharmacol. 4 (2006) 245–251.

[32] A. Jahangiri, M. Barzegar-Jalali, A. Garjani, Y. Javadzadeh, H. Hamishehkar, A. Afroozian, K. Adibkia, Pharmacological and histological examination of atorvastatin-PVP K30 solid dispersions, Powder Technol. 286 (2015) 538–545.

[33] C.L. Oltman, E.P. Davidson, L.J. Coppey, T.L. Kleinschmidt, D.D. Lund, M.A. Yorek, Attenuation of vascular/neural dysfunction in Zucker rats treated with enalapril or rosuvastatin, Obesity 16 (2008) 82–89.

[34] H.Y. Qu, Y.W. Xiao, G.H. Jiang, Z.Y. Wang, Y. Zhang, M. Zhang, Effect of ator-vastatin versus rosuvastatin on levels of serum lipids, inflammatory markers and adiponectin in patients with hypercholesterolemia, Pharm. Res. 26 (2009) 958–964.

[35] D. Festi, A. Colecchia, T. Sacco, M. Bondi, E. Roda, G. Marchesini, Hepatic steatosis in obese patients: clinical aspects and prognostic significance, Obes. Rev. 5 (2004) 27–42.

[36] S. Antonopoulos, S. Mikros, M. Mylonopoulou, S. Kokkoris, G. Giannoulis, Rosuvastatin as a novel treatment of non-alcoholic fatty liver disease in hyperlipi-demic patients, Atherosclerosis 184 (2006) 233–234.